



Article

Nonlinear Coupled Vibration Behavior of BFRP Cables on Long-Span Cable-Stayed Bridges under Parametric Excitation

Yaqiang Yang ^{1,*}, Zixian Zhou ¹, Yanlin Guan ¹, Jianzhe Shi ^{2,*}, Qiwei Zhan ¹ , Mohamed F. M. Fahmy ³ and Bitao Wu ⁴ 

¹ School of Architecture and Civil Engineering, Jiangsu University of Science and Technology, Zhenjiang 212100, China; 211110901104@stu.just.edu.cn (Z.Z.); 221210901109@stu.just.edu.cn (Y.G.); zhanqw@just.edu.cn (Q.Z.)

² College of Civil and Transportation Engineering, Hohai University, Nanjing 210098, China

³ Department of Civil Engineering, Faculty of Engineering, Assiut University, Assiut 71515, Egypt; m.fahmy@aun.edu.eg

⁴ School of Civil Engineering and Architecture, East China Jiao Tong University, Nanchang 330013, China; wubitao@ecjtu.edu.cn

* Correspondence: yangyq@just.edu.cn (Y.Y.); sjz@hhu.edu.cn (J.S.)

Abstract: Based on the cable-stayed beam model, this paper studies the nonlinear coupled vibration behavior of basalt fiber-reinforced polymer (BFRP) cables on long-span cable-stayed bridges under parametric excitation. Considering the sag, damping of BFRP cables, and the coupled interactions between stayed cables and the main girder, the nonlinear coupling vibration model of the BFRP cable-beam composite structure has been established. Taking the longest cable of Sutong Bridge as a case study, the nonlinear coupled vibration behavior of BFRP cables under parametric excitation has been numerically analyzed using the finite difference method. The analysis results indicate that (1) under parametric excitation, the large amplitude nonlinear vibration of the BFRP cable will be induced with an evident “beat” phenomenon. (2) Under the same parametric excitation, the nonlinear coupling vibration response and the beta frequency of the BFRP cable were both smaller than that of the traditional steel cable. (3) The nonlinear coupling vibration response of the BFRP cable increased with an increment in excitation amplitude and a decrement in cable force. With the increase in the excitation frequency, weight per unit length, and axial stiffness, the nonlinear vibration response of the BFRP cable increased first and then decreased. Meanwhile, the damping ratio of the BFRP cable had no significant influence on the nonlinear coupling vibration.

Keywords: BFRP cable; cable-beam composite structure; nonlinear coupled vibration; parametric excitation; long-span cable-stayed bridge



Citation: Yang, Y.; Zhou, Z.; Guan, Y.; Shi, J.; Zhan, Q.; Fahmy, M.F.M.; Wu, B. Nonlinear Coupled Vibration Behavior of BFRP Cables on Long-Span Cable-Stayed Bridges under Parametric Excitation. *Buildings* **2023**, *13*, 3082. <https://doi.org/10.3390/buildings13123082>

Academic Editor: Carmelo Gentile

Received: 16 October 2023

Revised: 30 November 2023

Accepted: 4 December 2023

Published: 11 December 2023



Copyright: © 2023 by the authors. Licensee MDPI, Basel, Switzerland. This article is an open access article distributed under the terms and conditions of the Creative Commons Attribution (CC BY) license (<https://creativecommons.org/licenses/by/4.0/>).

1. Introduction

With the increase in the span capacity of cable-stayed bridges, the disadvantages of traditional steel cables, including large self-weight, pronounced sag effect, and low carrying efficiency, have become more serious [1]. Due to the limitation of construction technology and economic performance, a main span of 1300 m has become the bottleneck of the long-span cable-stayed bridge [2]. In addition, the severe air pollution and increasing traffic load have aggravated the fatigue degradation and corrosion damage of the traditional steel cable, which cannot meet the requirements of the long-span cable-stayed bridge for long spans, long life, and high durability. It is necessary to develop a new material cable with superior mechanical and chemical properties and economic performance to apply on the long-span cable-stayed bridge to overcome the challenges in span and durability of bridge engineering [3]. Fiber-reinforced polymer (FRP for short) materials have been widely used in repairing existing structures and reinforcing new structures due to their high strength-to-weight ratio, good anti-fatigue properties, and superior corrosion resistance

during the past 30 years [4]. Manufacturing stayed cables with FRP materials can not only take full advantage of FRP materials such as high strength and lightweight qualities, good fatigue resistance, and superior anti-corrosion properties, but it also avoids the FRP material shortcomings of poor shearing performance. Therefore, the application of FRP cable on long-span cable-stayed bridges can increase span and service life significantly, which will provide an effective way to improve the short- and long-term performance of long-span cable-stayed bridges. Due to the superior mechanical and chemical properties, carbon fiber-reinforced polymer (CFRP for short) material has become the first choice for making FRP cables for long-span cable-stayed bridges [5]. However, the high cost and significant wind sensitivity of CFRP cable restrict its application on long-span cable-stayed bridges. Taking mechanical properties and economic performance into consideration, the feasibility of the other FRP materials used to manufacture FRP cables has been studied. Compared with the other FRP materials, basalt fiber-reinforced polymer (BFRP for short) has shown its mechanical and economic advantages, such as high strength, significant elongation, good fatigue resistance, superior anti-corrosion property, good chemical stability, and low cost [6]. With no emissions of harmful gases during manufacture, the BFRP cable has been regarded as one of the green inorganic fiber materials. With its outstanding advantages, theoretical and experimental studies on the mechanical behavior and structural performance of BFRP cables on long-span cable-stayed bridges have been carried out [7]. According to the existing studies [8], anchorage of BFRP cables with multiple tendons and large tonnage can be achieved using the anchorage method with a continuous fiber-reinforced load transfer component. Applying BFRP cable on long-span cable-stayed bridges can not only meet the requirement of bridge structure design but also reduce the axial force of the girder. In addition, BFRP cables can help to suppress the significant amplitude vibration of cables and optimize the economic performance of long-span cable-stayed bridges [9]. With the improvement in manufacturing and the accumulation of engineering experience, BFRP cables have broad prospects of application on long-span cable-stayed bridges.

With a quarter of the weight per unit length of the traditional steel cable, the BFRP cable is more sensitive to external excitation [10]. Under the same load excitation, the amplitude of vibration acceleration will be significantly larger than that of the steel cable [11], which shows the high sensitivity of the FRP cable under external excitation. According to existing studies [12,13], the large-amplitude vibration of the stayed cable will be induced under parametric excitation, whose excitation frequency is twice the natural frequency of the stayed cable. However, the results of the analysis for the stayed cable do not agree with the actual vibration behavior on long-span cable-stayed bridges due to the overlooking of the coupled vibration interaction between the cable and the deck of the long-span cable-stayed bridge. It is necessary to analyze the parametric vibration behavior of the FRP cable on a long-span cable-stayed bridge considering the coupled vibration interaction. For the cable-stayed bridges, masts, and suspended roofs, the cable-stayed beam model has been widely adopted in coupled vibration analysis. Through a mass block [14], simply supported beam [15], or cantilever beam [16] simulating the bridge deck, reduced cable–beam models were employed to study the nonlinear coupled behavior of the stayed cable on a long-span cable-stayed bridge. Based on the cable-stayed beam model, the coupled vibration responses were constructed with their vibration characteristics, influence factors, and the coupling effects on the cable. With the reduced cable–beam model (cable–mass block model), Guo [17,18] investigated the cable’s forced nonlinear vibration that was excited by beam oscillation and numerically analyzed the influence of the deck/cable mass ratio, cable inclination, boundary damping, and internal detuning on the nonlinear vibration responses. According to the cable–simple support beam model, Kang [19] and Cong [20] explored the spatial dynamic theory and analyzed the multimodal interaction of the system, which deduced a wealth of behavior from the results, including the saddle-node bifurcation, Hopf bifurcation, and veering phenomenon. Based on the cable–cantilever beam, Cong [21] clarified that the cable experienced a more significant response than the beam, whether excitations were applied to the beam or the cable. In addition, Mohammad [22] discussed

the effect of bending stiffness and sag of the cable on the system dynamics through theoretical analysis and vibration experiments. With regard to the numerical simulation methods for reproducing the nonlinear behavior of cable elements, there are various numerical strategies such as the multi-truss element approach and the catenary element model. Using the multi-truss element approach, Lonetti [23] proposed a numerical model for predicting the structural integrity of a self-anchored cable-stayed suspension bridge considering both geometric and material nonlinearities. With the catenary element model, Zhou [24] numerically assessed the load effects on the prototype of a long-span cable-stayed bridge and revealed that the design live load from AASHTO may be unsafe for use as the live load. Although phase achievements in the nonlinear vibration behavior of the cable–beam composite structure have been made, the coupled effect between the stayed cable and the beam has not been taken into full consideration, resulting in an inaccurate description of the parametric vibration behavior of the stayed cables. Meanwhile, the existing studies of parametric vibration cannot be directly applied to BFRP cables due to the changing conditions of nonlinear vibration and the complex mechanism of damping the dissipation energy of BFRP cables. It is necessary to establish the nonlinear coupling vibration model of the BFRP cable–beam composite structure to study the nonlinear vibration behaviors of BFRP cables on the long-span cable-stayed bridges under parametric excitation. Taking the nonlinear factors of BFRP cables and coupling effects between the stayed cable and beam into consideration, this paper proposed the nonlinear coupled vibration model. It carried out the theoretical and numerical studies of BFRP cables on the long-span cable-stayed bridges under parametric excitation. To better understand the nonlinear parametric vibration of BFRP cables, the key influencing factors of the nonlinear vibration behavior of BFRP cables on long-span cable-stayed bridges under parametric excitation have been discussed in this paper.

2. Nonlinear Coupling Vibration Model of the BFRP Cable–Beam

In cable-stayed bridges, the vibration behaviors of stayed cables are usually influenced by the girder and the tower. Compared with the girder, the impact of the tower on stayed cables can be negligible due to the significant stiffness of the tower. As shown in Figure 1, the cable–beam model has been employed to study the nonlinear coupling vibration behavior of the BFRP cables on long-span cable-stayed bridges [25]. According to the Cartesian coordinate system, the vibration of the girder and stayed cable can be described by $O_c X_c Z_c$ and $O_b X_b Z_b$ in the coordinates of the cable–beam model, where w_c and u_c indicate the in-plane and axial displacement of BFRP cable, respectively, and w_b and u_b imply the in-plane and axial displacement of the girder, respectively. By ignoring the secondary factors, the following basic assumptions were proposed to study the nonlinear vibration of BFRP cables on long-span cable-stayed bridges:

- (1) During the whole vibration process of the cable–beam composite structure, the BFRP cable and girder are in a linear elastic state;
- (2) Under the effect of gravity, the structural configuration of the BFRP cable can be described by the parabolic equation. Taking the sag into consideration, the structural shape of the BFRP cable can be indicated as in Equation (1), in which m_c and H_c represent the mass per unit length and cable force of the BFRP cable, respectively; x_c and z_c represent the axial and transverse coordinates of the BFRP cable in the $O_c X_c Z_c$ Cartesian coordinate system; g denotes the gravity acceleration; θ indicates the angle between the girder and the stayed cable; l_c and l_b imply the length of the girder and of the BFRP cable, respectively;

$$z_c(x_c) = \frac{m_c g \cos \theta}{2H_c} x_c(l_c - x_c) \quad (1)$$

- (3) Compared with transverse acceleration and axial stiffness, the axial acceleration, shear stiffness, torsional stiffness, and flexural stiffness of the BFRP cable have no

significant influence on the nonlinear vibration behaviors, which can be ignored during the analysis;

- (4) Due to the small axial and shear deformation, only the flexural deformation of the girder has been taken into consideration.

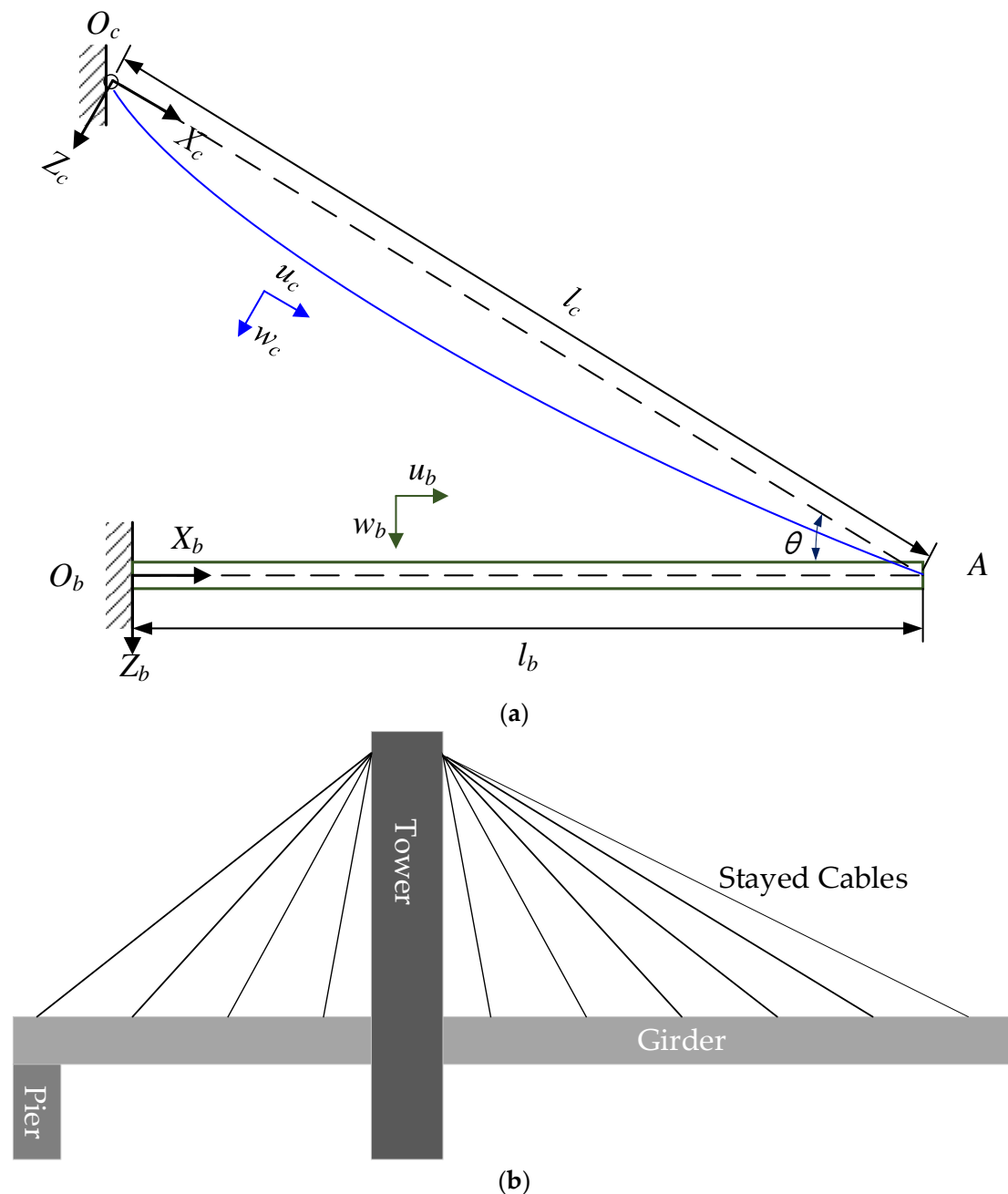


Figure 1. Cable-beam composite structure: (a) model structure; (b) actual structure.

Based on the above assumptions, the nonlinear vibration differential equation of the BFRP cable and girder can be established according to the D'Alembert principle. As shown in Equations (2) and (3), $w_c(x_c, t)$ and w_b denote the transverse vibration displacement of the BFRP cable and the vibration displacement of the girder, respectively; $E_c A_c$ and $E_b I_b$ represent the axial stiffness of the BFRP cable and the flexural stiffness of the girder; f_c and f_b represent the distribution load of the BFRP cable and the girder, respectively; c_c and c_b indicate the damping coefficients of the BFRP cable and the girder, respectively; m_b and

x_b imply the mass per unit length and transverse coordinates the in $O_bX_bZ_b$ system of the girder, respectively; L_e states the virtual length of the BFRP cable.

$$m_c \frac{\partial^2 w_c}{\partial t^2} + c_c \frac{\partial w_c}{\partial t} - H_c \frac{\partial^2 w_c}{\partial x_c^2} + \frac{E_c A_c}{L_e} \left(\frac{m_c g \cos \theta}{H_c} \right)^2 \int_0^{l_c} w_c dx_c + \frac{E_c A_c}{L_e} \frac{m_c g \cos \theta}{H_c} \cdot \int_0^{l_c} \left(\frac{\partial w_c}{\partial x_c} \right)^2 dx_c - \frac{E_c A_c}{L_e} \left[u_c(l_c) - \frac{m_c g l_c \cos \theta}{2 H_c} w_c(l_c) + \frac{m_c g \cos \theta}{H_c} \int_0^{l_c} w_c dx \right] \frac{\partial^2 w_c}{\partial x_c^2} \quad (2)$$

$$= f_c - \frac{E_c A_c}{L_e} \frac{m_c g \cos \theta}{H_c} \left[u_c(l_c) - \frac{m_c g l_c \cos \theta}{2 H_c} w_c(l_c) \right]$$

$$m_b \frac{\partial^2 w_b}{\partial t^2} + c_b \frac{\partial w_b}{\partial t} + H_c \cos \theta \frac{\partial^2 w_b}{\partial x_b^2} + E_b I_b \frac{\partial^4 w_b}{\partial x_b^4} = f_b \quad (3)$$

To obtain the nonlinear vibration responses, the boundary condition and displacement continuous condition of the BFRP cable and the girder should be proposed based on the cable–beam composite model.

Compared with only considering the vibration behavior of the BFRP cable, the coupling interaction between the BFRP cable and the girder has a significant influence on the nonlinear vibration responses of the BFRP cable–beam composite structure, which can result in changes in the cable force and in the displacement/rotation between the girder and BFRP cable end. Therefore, the nonlinear vibration differential equation of the BFRP cable–beam composite structure should also satisfy the dynamic equilibrium condition induced by the above coupling interaction, expressed in Equation (4), in which h_c represents the additional cable force generated during the nonlinear vibration of BFRP cable, and φ_{c0} denotes the initial rotation of the BFRP cable end.

$$E_b I_b \frac{\partial^3 w_b}{\partial x_b^3}(l_b) = h_c (\sin \theta - \cos \theta \tan \varphi_{c0}) - H_c \frac{\partial w_b}{\partial x_b} \cos \theta + H_c \frac{\partial w_c}{\partial x_c} \cos \theta \quad (4)$$

To simplify the nonlinear vibration analysis, dimensionless parameters were introduced. Based on the finite difference method, the numerical algorithm of the nonlinear coupling vibration response of the cable–beam composite structure was proposed and is shown in Figure 2.

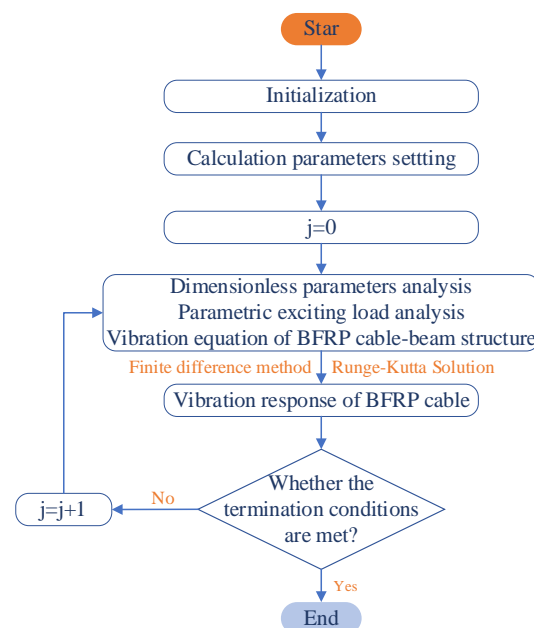


Figure 2. Algorithmic program of nonlinear coupling vibration response for BFRP cable–beam model.

3. Nonlinear Vibration Study of BFRP Cable–Beam Composite Structures under Parametric Excitation

Based on the above nonlinear coupling vibration model, the longest stayed cable on the Sutong Bridge in China, shown in Figure 3, was selected as an example to discuss the nonlinear coupling vibration behavior of the BFRP cable on a long-span cable-stayed bridge under parametric excitation [26]. Compared to short cables, the nonlinear coupling vibration of the long cable has significant effects on the dynamic performance of the long-span cable-stayed bridge. Therefore, the longest stayed cable of Sutong Bridge was taken as the research object. In Table 1, the structural parameters of the prototype cable have been listed. Through considering mechanical properties and economic performance [27], the section parameter of the BFRP cable was designed in terms of the strength principle, as shown in Equation (5), in which $F_{d,S}$ and $F_{d,B}$ denote the design cable force of the steel cable and the BFRP cable, respectively; $f_{s,B}$ represents the tensile strength of the material design strength of the cable; S_B and A_B indicate safety factor and sectional area of the BFRP cable, respectively. The structural parameters of the BFRP cable are also listed in Table 1.

$$\{F_{d,B} = F_{d,S}; f_{d,B} = \frac{f_{s,B}}{S_B}; A_B = \frac{F_{d,B}}{f_{d,B}}\} \Rightarrow A_B = \frac{F_{d,B} \cdot S_B}{f_{s,B}} \quad (5)$$

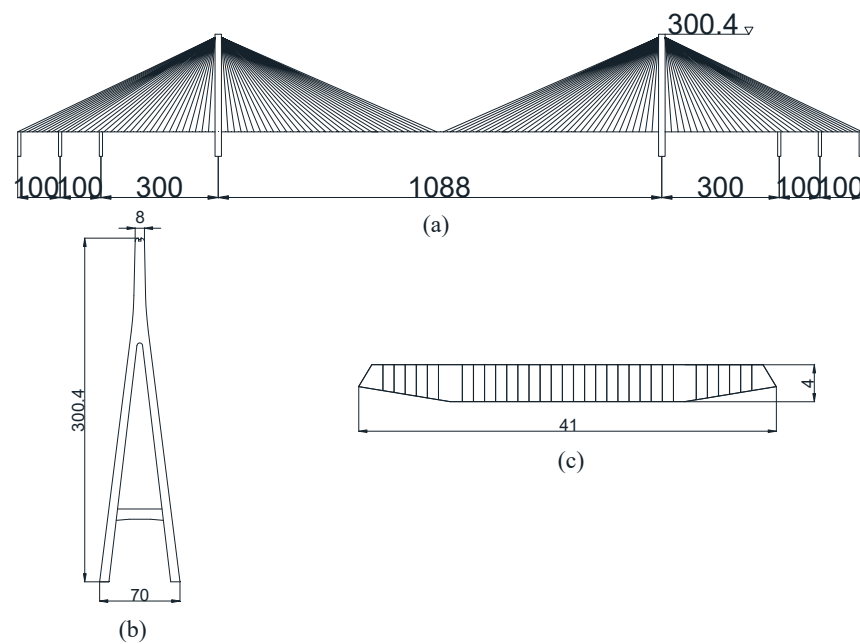


Figure 3. Sutong Bridge structure diagram: (a) layout of the whole bridge; (b) tower; (c) girder.

Table 1. Parameter of material and structure of steel cable and BFRP cable.

Cable Type	Density (kg/m ³)	Length (m)	Inclination (°)	Elastic Modulus (GPa)	Tensile Strength (MPa)	Safety Factor	Design Cable Force (10 ⁷ N)	Sectional Area (10 ^{−2} m ²)	Damping Ratio (%)	Natural Frequency (Hz)
HS	7850	576	23	210	1860	2.5	1.19	1.89	0.17	0.25
BFRP	1739	576	23	58.23	1470	4.0	1.19	3.24	0.78	0.40

In Table 1, the natural frequency (ω) of the stayed cable can be derived based on the theoretical formula for string vibration, as shown in Equation (6). Meanwhile, the experimental results of the damping ratios of the steel cable and the BFRP cable were adopted in this analysis [25]. As shown in Figure 3, the girder of the Sutong Bridge is the

steel box beam made of Q345 and Q370 grade steel, whose sectional parameters are listed in Table 1.

$$\omega = \frac{1}{2l_c} \sqrt{\frac{H_c}{m_c}} \quad (6)$$

Once the exciting frequency from the external environment achieves twice the natural frequency of the stayed cable, the large-amplitude parametric vibration of the cable will be induced. Therefore, the nonlinear vibration behavior of the BFRP cable on the long-span cable-stayed bridge under parametric excitation was studied by applying harmonic loads with the twice the natural frequency of the stayed cable, which can be expressed using dimensionless parameters such as $f_c = 0, f_b = 10^{-5} \sin(\pi x_b) \cos(2t)$. Based on the proposed numerical algorithm, the nonlinear vibration response of the steel cable and the BFRP cable has been analyzed. As shown in Figure 4, the displacement–time curves of the midpoint and endpoint of the BFRP cable under parametric excitation are compared with that of the traditional steel cable. It indicates that a significant amplitude vibration can be induced by parametric excitation both for the steel cable and the BFRP cable. In addition, there are apparent beating vibration phenomena during the nonlinear vibration process of the steel cable and the BFRP cable. Furthermore, the vibration response of the midpoint is more significant than that of the endpoint both for the steel cable and the BFRP cable under parametric excitation. However, the parametric vibration amplitudes of the midpoint and endpoint of the BFRP cable are about 44% and 8% less than that of the steel cable, respectively, as shown in Table 2. Furthermore, the frequency of the beat vibration of the BFRP cable is lower than that of the steel cable. In addition, the beat vibration of the steel cable maintained a presence and had no fundamental amplitude decay or frequency decay under the parametric excitation. However, the beat frequency of the BFRP cable decreased gradually with the increase in parametric excitation. With the reduction in the vibration amplitude, the parametric vibration of the BFRP cable decayed to a steady amplitude. This is because the BFRP cable as a composite material is endowed with viscoelastic properties and vibration absorption. To sum up, applying BFRP cables on long-span cable-stayed bridges can effectively reduce the parametric vibration response and improve the vibration stability of the stayed cable under the parametric excitation.

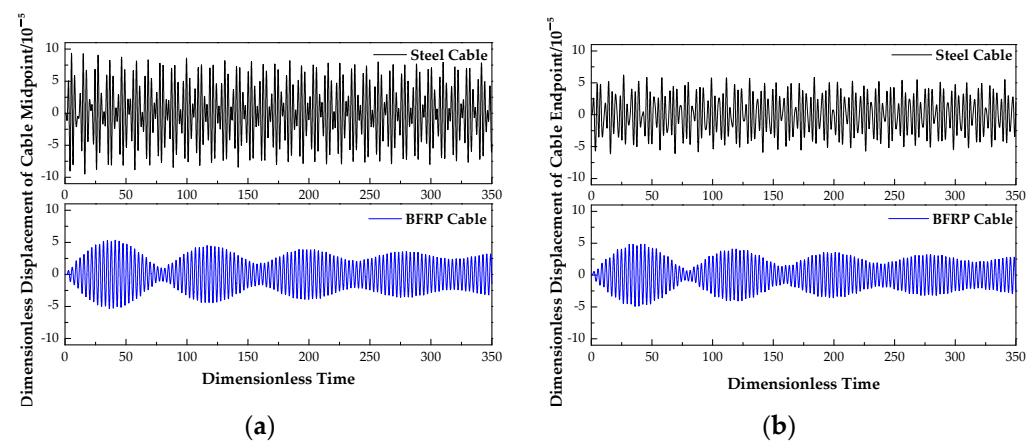


Figure 4. Nonlinear coupled vibration response of steel cable and BFRP cable under parametric excitation: (a) displacement–time curves of midpoint of stayed cable; (b) displacement–time curves of endpoint of stayed cable.

Table 2. Maximum amplitude of steel cable and BFRP cable under parametric excitation.

Cable Type	Midpoint ($\times 10^{-5}$)	Endpoint ($\times 10^{-5}$)
Steel Cable	9.46	5.34
BFRP Cable	5.34	4.91

4. Analysis of Influence Factors

According to the nonlinear coupling vibration model of the BFRP cable–beam, the factors that influence the parametric vibration behavior of the BFRP cable include the frequency and amplitude of the external excitation, the mass per unit length, the damping ratio, the axial stiffness, and the cable force of the BFRP cable. To explore the critical factors that influence the regularity of the parametric vibration behavior of the BFRP cable, the nonlinear coupling vibration behavior of the BFRP cable under parametric excitation has been studied by changing the influencing factors and conducting numerical analysis.

4.1. Excitation Frequency

Keeping the other parameters unchanged, the nonlinear coupling vibration responses of the midpoint and endpoint of the BFRP cable was obtained under three different excitation frequencies, which were applied on the BFRP cable–beam composite structure and expressed using dimensionless parameters such as $f_c = 0, f_b = 10^{-5} \sin(\pi x_b) \cos(t)$; $f_c = 0, f_b = 10^{-5} \sin(\pi x_b) \cos(2t)$; $f_c = 0, f_b = 10^{-5} \sin(\pi x_b) \cos(3t)$. As shown in Figure 5, the nonlinear coupling vibration responses of the BFRP cable under different excitation frequencies are compared. It can be seen from Figure 5 that the vibration amplitude of the BFRP cable first increases and then decreases with the increase in the excitation frequency. In particular, the vibration amplitude achieves the maximum value (5.34×10^{-5} or 4.91×10^{-5}) with the most obvious beat vibration when the excitation frequency is twice the natural frequency of the BFRP cable, as shown in Figure 5 and Table 3. This is because the external excitation will continuously input vibration energy and focus on the cable vibration when the excitation frequency is twice the natural frequency. In addition, the maximum vibration amplitude of the BFRP cable exciting at three times the natural frequency was about 30% less than that excited by the natural frequency, as shown in Table 3. Moreover, there was no significant beat vibration once the BFRP cable was excited by natural frequency and triple natural frequency, excluding the vibration responses of the midpoint of the BFRP cable under triple natural frequency. In conclusion, it is prone to induce a large-amplitude parametric vibration for the BFRP cable when the excitation frequency reaches twice the natural frequency of the BFRP cable. Therefore, effective measures should be taken to suppress the large-amplitude parametric vibration.

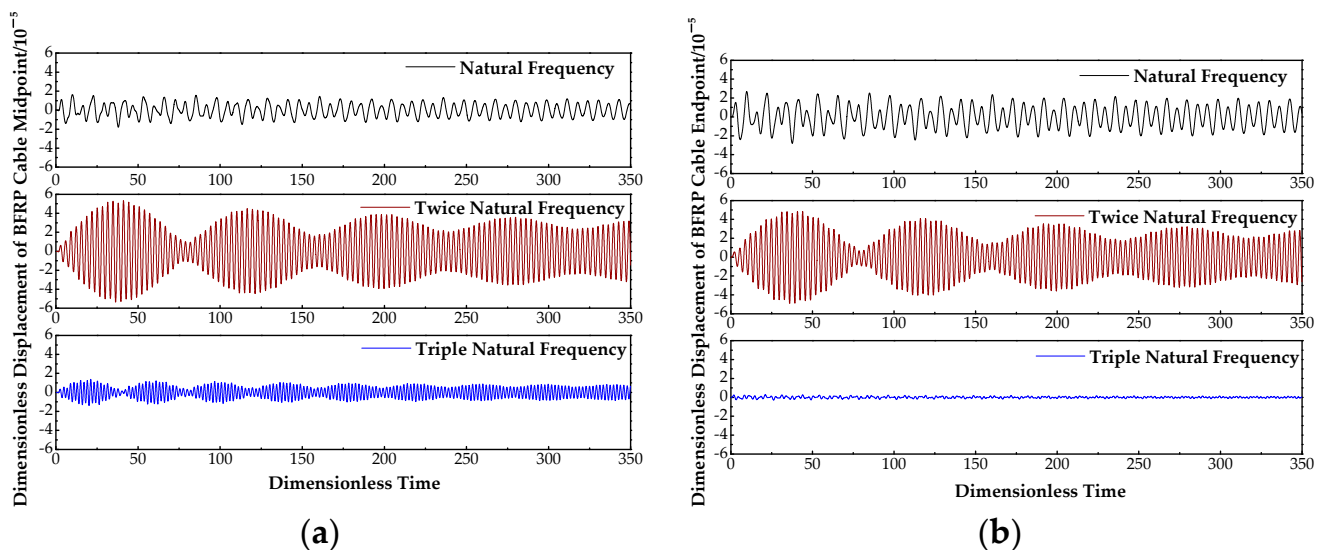


Figure 5. Nonlinear coupled vibration response of BFRP cable under parametric excitation with different frequencies: (a) nonlinear vibration response of midpoint; (b) nonlinear vibration response of endpoint.

Table 3. Maximum amplitude of BFRP cable with different frequencies.

Frequency	Midpoint ($\times 10^{-5}$)	Endpoint ($\times 10^{-5}$)
$f_c = 0, f_b = 10^{-5} \sin(\pi x_b) \cos(t)$	1.79	2.80
$f_c = 0, f_b = 10^{-5} \sin(\pi x_b) \cos(2t)$	5.34	4.91
$f_c = 0, f_b = 10^{-5} \sin(\pi x_b) \cos(3t)$	1.37	2.97

4.2. Excitation Amplitude

At the parametric excitation frequency (twice the natural frequency), the excitations with different amplitudes were applied to the BFRP cable–beam composite structure as the input loads to discuss the influence of the excitation amplitude on the parametric vibration response of the BFRP cable. There were three—large, medium, and small—amplitude parametric excitations separately acting on the BFRP cable–beam model, which can be referred to, respectively, as $f_c = 0, f_b = 5 \times 10^{-6} \sin(\pi x_b) \cos(2t)$; $f_c = 0, f_b = 10^{-5} \sin(\pi x_b) \cos(2t)$; and $f_c = 0, f_b = 2 \times 10^{-5} \sin(\pi x_b) \cos(2t)$ according to dimensionless parameters. The parametric vibration responses of the midpoint and endpoint on the BFRP cable under different vibration amplitudes are compared in Figure 6 and Table 4. As shown in Figure 6, the parametric vibration responses of the BFRP cable increased with the increase in the excitation amplitude. In addition, an increment in the maximum amplitude of the BFRP cable was nearly the same as that of the excitation amplitude as shown in Table 4. Furthermore, it would take more time for the BFRP cable to achieve a stable vibration amplitude when the excitation amplitude increased. Consequently, more attention should be paid to the large-amplitude parametric vibration of the BFRP cable used on long-span cable-stayed bridges.

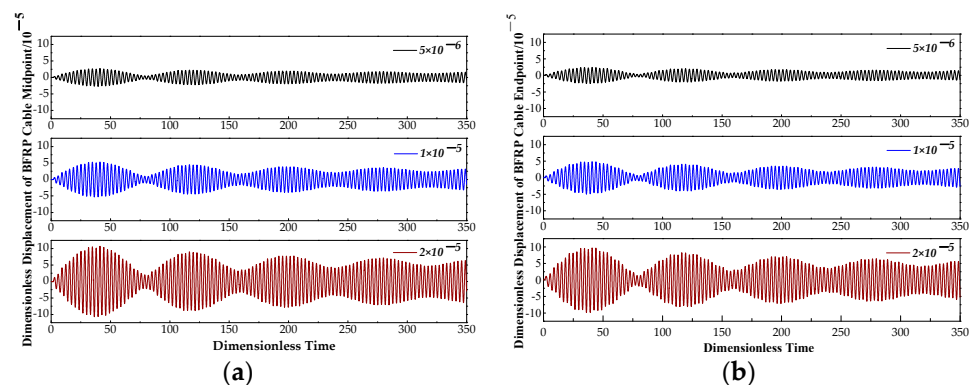


Figure 6. Nonlinear coupled vibration response of BFRP cable under parametric excitation with different vibration amplitudes: (a) nonlinear vibration response of the midpoint; (b) nonlinear vibration response of the endpoint.

Table 4. Maximum amplitude of BFRP cable with different vibration amplitudes.

Vibration Amplitude	Midpoint ($\times 10^{-5}$)	Endpoint ($\times 10^{-5}$)
$f_c = 0, f_b = 5 \times 10^{-6} \sin(\pi x_b) \cos(2t)$	2.67	2.46
$f_c = 0, f_b = 10^{-5} \sin(\pi x_b) \cos(2t)$	5.34	4.91
$f_c = 0, f_b = 2 \times 10^{-5} \sin(\pi x_b) \cos(2t)$	10.69	9.82

4.3. Section Parameters

For stayed cable, the section parameter, such as mass per unit length or axial stiffness, changes with the section area of the cable. Proportional to the section area, the mass per unit length and axial stiffness of the BFRP cable increase according to the section area of the BFRP cable. By changing the section area of the BFRP cable, the effects of mass per unit length and axial stiffness on the nonlinear coupling vibration behavior of the BFRP cable can be studied. Three representative sections of the BFRP cable were used to discuss the vibration

response of the BFRP cable under parametric excitation, which involved $2.43 \times 10^{-2} \text{ m}^2$, $3.24 \times 10^{-2} \text{ m}^2$, and $4.05 \times 10^{-2} \text{ m}^2$. The parametric vibration–time history curves of the BFRP cable with different section areas are shown in Figure 7 and Table 5. It is indicated from Figure 7 and Table 5 that the vibration amplitude of the BFRP cable under parametric excitation increased and then decreased with the increase in the mass per unit length and axial stiffness of the cable. However, with a rise in the mass per unit length and axial stiffness of the cable, the frequency of the beat vibration of the BFRP cable under parametric excitation decreased firstly and then increased. As the ratio of the mass per unit length and axial stiffness of the BFRP cable approximates 1:1.3:1.7, the ratio of the beat vibration frequency of the BFRP cable under parametric excitation approaches 4:1:2.

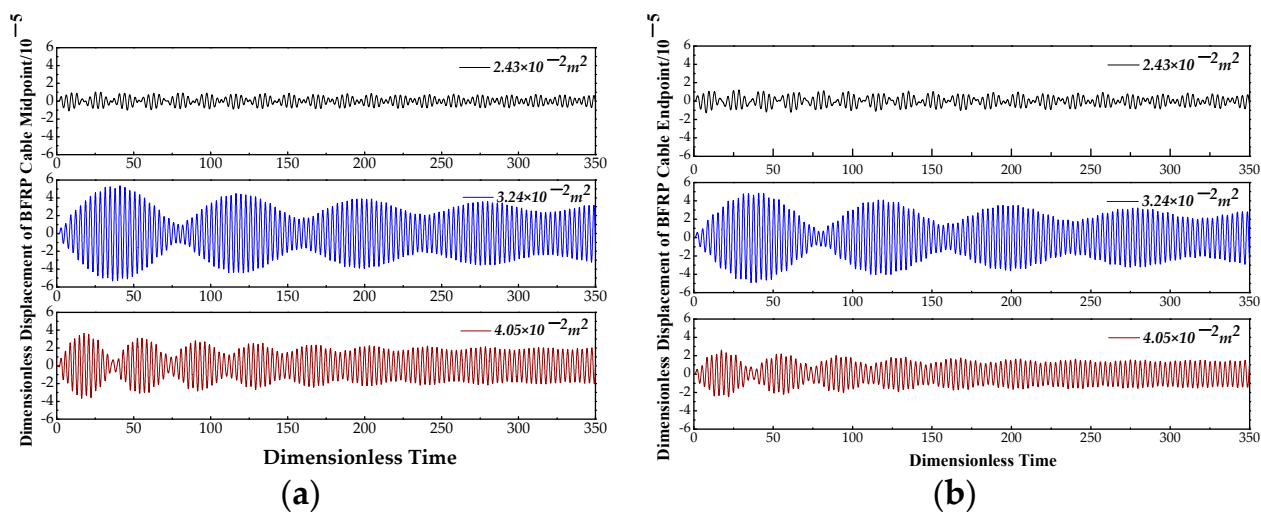


Figure 7. Nonlinear coupled vibration response of BFRP cable under parametric excitation at different section areas: (a) nonlinear vibration response of the midpoint; (b) nonlinear vibration response of the endpoint.

Table 5. Maximum amplitude of BFRP cable at different section areas.

Section Area	Midpoint ($\times 10^{-5}$)	Endpoint ($\times 10^{-5}$)
$2.43 \times 10^{-2} \text{ m}^2$	1.11	1.28
$3.24 \times 10^{-2} \text{ m}^2$	5.34	4.91
$4.05 \times 10^{-2} \text{ m}^2$	3.66	2.61

4.4. Cable Force

As one of the critical influencing factors, variation in the cable force would have significant effects on the vibration behavior of the BFRP cable. Under the condition of constant parametric excitation, the nonlinear vibration responses of the BFRP cable were analyzed by applying large, medium, and small cable forces, which were $1.01 \times 10^7 \text{ N}$, $1.19 \times 10^7 \text{ N}$, and $1.37 \times 10^7 \text{ N}$, respectively. The results of the analysis of the midpoint and endpoint of the BFRP cable with different cable forces are compared in Figure 8 and Table 6. As shown in Figure 8 and Table 6, the nonlinear parametric vibration response of the midpoint of the BFRP decreased with the increase in the cable force. For the parametric vibration of the endpoint of the BFRP cable when applying different cable forces, it increased slightly initially and decreased obviously afterward as shown in Table 6. However, the beat frequency of the parametric vibration of the BFRP cable decreased at first and then increased with the increase in the cable force both for the midpoint and the endpoint of the cable, as shown in Figure 8.

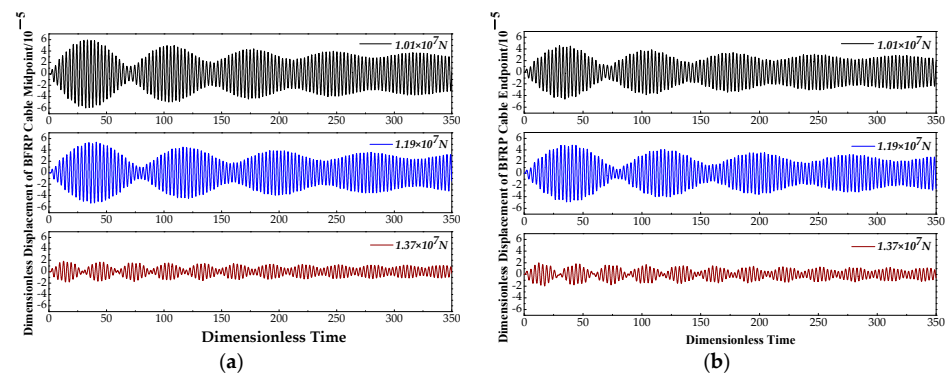


Figure 8. Nonlinear coupled vibration response of BFRP cable under parametric excitation with different cable forces: (a) nonlinear vibration response of the midpoint; (b) nonlinear vibration response of the endpoint.

Table 6. Maximum amplitude of BFRP cable with different cable forces.

Cable Force	Midpoint ($\times 10^{-5}$)	Endpoint ($\times 10^{-5}$)
1.01×10^7 N	5.94	4.61
1.19×10^7 N	5.34	4.91
1.37×10^7 N	1.84	1.99

4.5. Damping Ratio

As a key factor in vibration attenuation and energy dissipation, damping ratio has an essential influence on the nonlinear vibration behavior of the stayed cable on long-span cable-stayed bridges. To study the influence regularity of damping ratio on the parametric vibration behavior, BFRP cables with three different damping ratios relating to 7.8×10^{-4} , 7.8×10^{-3} , and 7.8×10^{-2} were employed to carry out the nonlinear vibration analysis. Under similar parametric excitation, the vibration time–history responses of the BFRP cable with different damping ratios are compared in Figure 9. It can be seen from Figure 9 that there were no significant differences in the parametric vibration amplitude and frequency of the midpoint and endpoint of the BFRP cable with different inherent damping ratios as shown in Table 7. Once the large amplitude parametric vibration is induced, the intrinsic damping ratio has no significant effect on suppressing the nonlinear vibration of the BFRP cable under parametric excitation. It is necessary to install additional dampers to control the large-amplitude parametric vibration for the BFRP cable on long-span cable-stayed bridges.

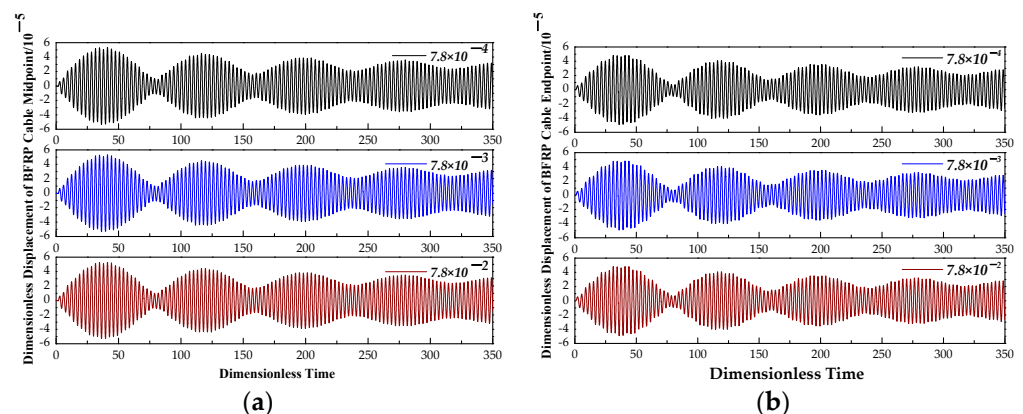


Figure 9. Nonlinear coupled vibration response of BFRP cable under parametric excitation with different damping ratios: (a) nonlinear vibration response of the midpoint; (b) nonlinear vibration response of the endpoint.

Table 7. Maximum amplitude of BFRP cable with different damping ratios.

Damping Ratio	Midpoint ($\times 10^{-5}$)	Endpoint ($\times 10^{-5}$)
7.8×10^{-4}	5.35	4.91
7.8×10^{-3}	5.34	4.91
7.8×10^{-2}	5.29	4.90

Based on the analysis of the influencing factors of the parametric vibration behavior of the BFRP cable under parametric excitation, the external excitation and mechanical characteristics of BFRP cables have significant effects on the nonlinear coupled vibration of BFRP cables on long-span cable-stayed bridges. Therefore, effective measures should be taken to suppress the nonlinear coupled vibration of BFRP cables once applied on long-span cable-stayed bridges in the future. On the one hand, the girder section and restriction damping of the cable-stayed bridges should be properly designed to change the natural frequency and amplitude of the girder, which could help BFRP cables avoid the natural frequency and amplitude of parametric vibration. On the other hand, the external damper and cross-tie cable should be applied on BFRP cables to improve the mechanical performance including the free length, natural frequency, and stiffness of the cable system, which could reduce the response of the parametric vibration.

5. Conclusions

Based on the cable–beam composite structure, the nonlinear coupling vibration model of BFRP cables on long-span cable-stayed bridges was proposed. The longest-stayed cable of the Sutong Bridge was taken as a case study to investigate the nonlinear coupling vibration behavior of the BFRP cable under the parametric excitation according to the BFRP cable–beam model. Through influence parameter analysis, the vibration regulations of the BFRP cable under parametric excitation were studied. Based on these analyses, the following major conclusions were drawn:

- (1) Under parametric excitation, large-amplitude and significant beat vibration would be induced both for the steel cable and the BFRP cable. However, the frequency of the parametric vibration of the BFRP cable was considerably less than that of the steel cable. Furthermore, the maximum amplitude of the BFRP cable was up to 44% less than that of the steel cable due to superior mechanical performance.
- (2) The maximum vibration amplitude with evident beat vibration would be obtained once the excitation frequency is twice the natural frequency of the BFRP cable. In addition, the larger the excitation amplitude was, the greater the nonlinear parametric vibration responses of the BFRP cable became. The increment in the maximum amplitude of the BFRP cable was nearly the same as that of the excitation amplitude.
- (3) With an increase in the mass per unit length and axial stiffness, the vibration amplitude of the BFRP cable under parametric excitation increased firstly and then decreased, while the frequency of the beat vibration decreased firstly and then increased.
- (4) The nonlinear parametric vibration response of the BFRP decreased with an increase in the cable force. The inherent damping ratio of the BFRP cable had no significant influence on the parametric vibration behavior.
- (5) Parametric vibration control has become the key issue for the application of BFRP cables on long-span cable-stayed bridges. Establishing parametric vibration control theory and developing parametric vibration control methods will be the development direction of future research.

Author Contributions: Conceptualization, Y.Y. and Z.Z.; methodology, Y.Y. and B.W.; software, Y.Y., Q.Z. and Y.G.; validation, Y.Y., Z.Z. and M.F.M.F.; formal analysis, Y.Y.; investigation, Y.Y. and B.W.; resources, Y.Y. and Q.Z.; data curation, Y.Y.; writing—original draft preparation, Y.Y.; writing—review and editing, Y.Y. and M.F.M.F.; visualization, Y.Y. and J.S.; supervision, Y.Y.; project administration, Y.Y.; funding acquisition, Y.Y., Q.Z. and J.S. All authors have read and agreed to the published version of the manuscript.

Funding: This research was funded by National Natural Science Foundation of China (Grant Number 51808265); Natural Science Foundation of the Jiangsu Higher Education Institutions of China (Grant Number 18KJB560005); Key Research and Development of Shandong Province (Grant Number 2019GSF111013); Postgraduate Research & Practice Innovation Program of Jiangsu Province (Grant Number 1122162210); and Key Research & Development Project of Zhenjiang City (Industry Foresight and Common Key Technologies) (Grant Number GY2023028).

Data Availability Statement: The data presented in this study are available in the article.

Conflicts of Interest: The authors declare no conflict of interest.

References

- Wang, Z.; Xian, G. Impact performances of fiber reinforced polymer composites and cables: A review. *Compos. Struct.* **2023**, *319*, 117128. [\[CrossRef\]](#)
- Wu, Z.; Liu, J.; Zou, D.; Wang, X.; Shi, J. Status and Development Trend of Light-Weight, High-Strength, and Durable Structural Materials Applied in Marine Bridge Engineering. *Strateg. Study CAE* **2019**, *21*, 31–40. [\[CrossRef\]](#)
- Guo, R.; Li, C.; Xian, G. Water absorption and long-term thermal and mechanical properties of carbon/glass hybrid rod for bridge cable. *Eng. Struct.* **2023**, *274*, 601–617. [\[CrossRef\]](#)
- Wei, Y.; Bai, J.; Zhang, Y.; Miao, K.; Zheng, K. Compressive performance of high-strength seawater and sea sand concrete-filled circular FRP-steel composite tube columns. *Eng. Struct.* **2021**, *240*, 112357. [\[CrossRef\]](#)
- Zhou, J.; Wang, X.; Ding, L.; Liu, S.; Wu, Z. Numerical and Experimental Study on Large-Diameter FRP Cable Anchoring System with Dispersed Tendons. *Buildings* **2023**, *13*, 92. [\[CrossRef\]](#)
- Macro, D.; Nicola, N. A Split-Wedge Anchorage for CFRP Cables: Numerical Model vs. Experimental Results. *Polymers* **2022**, *14*, 2675. [\[CrossRef\]](#)
- Yang, Y.; Fahmy, M.F.M.; Guan, S.; Pan, Z.; Zhan, Y.; Zhao, T. Properties and applications of FRP cable on long-span cable-supported bridges: A review. *Compos. Part B Eng.* **2020**, *190*, 107934. [\[CrossRef\]](#)
- Shi, J.; Wang, X.; Zhang, L.; Wu, Z.; Zhu, Z. Composite-Wedge Anchorage for Fiber-Reinforced Polymer Tendons. *J. Compos. Constr.* **2022**, *26*, 04022005. [\[CrossRef\]](#)
- Zhou, J.; Wang, X.; Peng, Z.; Wu, Z.; Wei, X. Enhancement of FRP Cable Anchor System: Optimization of Load Transfer Component and Full-Scale Cable Experiment. *J. Compos. Constr.* **2022**, *26*, 801–815. [\[CrossRef\]](#)
- Kim, T.; Jung, W. Improvement of Anchorage Performance of Carbon Fiber-Reinforced Polymer Cables. *Polymer* **2022**, *14*, 1239. [\[CrossRef\]](#)
- Yang, Y.; Fahmy, M.F.M.; Pan, Z.; Guan, S.; Zhan, Y. Analytical estimation on damping behaviors of the Self-Damping fiber reinforced polymer (FRP) cable. *Structures* **2020**, *25*, 774–784. [\[CrossRef\]](#)
- Wang, X.; Wu, Z. Vibration control of different FRP cables in long-span cable-stayed bridge under indirect excitations. *J. Earthq. Tsunami* **2011**, *5*, 167–188. [\[CrossRef\]](#)
- Mei, K.H.; Lu, Z.T.; Sun, S.J. Property of Nonlinear Parametric Vibration of CFRP Cables. *China J. Highw. Transp.* **2007**, *17*, 43–45.
- Guo, T.; Kang, H.; Wang, L.; Zhao, Y. An asymptotic expansion of cable-flexible support coupled nonlinear vibrations using boundary modulations. *Nonlinear Dyn.* **2017**, *88*, 33–59. [\[CrossRef\]](#)
- Su, X.; Kang, H.; Guo, T.; Cong, Y. Dynamic analysis of the in-plane free vibration of a multi-cable-stayed beam with transfer matrix method. *Arch. Appl. Mech.* **2019**, *89*, 31–48. [\[CrossRef\]](#)
- Wang, L.; Zhang, X.; He, K.; Peng, J. Revisited dynamic modeling and eigenvalue analysis of the cable-stayed beam. *Acta Mech. Sin.* **2020**, *36*, 950–963. [\[CrossRef\]](#)
- Guo, T.; Kang, H.; Wang, L.; Zhao, Y. An inclined cable excited by a non-ideal massive moving deck: An asymptotic formulation. *Nonlinear Dyn.* **2019**, *95*, 749–767. [\[CrossRef\]](#)
- Guo, T.; Kang, H.; Wang, L.; Zhao, Y. Cable dynamics under non-ideal support excitations: Nonlinear dynamic interactions and asymptotic modelling. *J. Sound Vib.* **2016**, *384*, 253–272. [\[CrossRef\]](#)
- Kang, H.; Guo, T.; Zhu, W. Multimodal interaction analysis of a cable-stayed bridge with consideration of spatial motion of cables. *Nonlinear Dyn.* **2020**, *99*, 123–147. [\[CrossRef\]](#)
- Cong, Y.; Kang, H.; Guo, T. Planar multimodal 1:2:2 internal resonance analysis of cable-stayed bridge. *Mech. Syst. Signal Process.* **2019**, *120*, 505–523. [\[CrossRef\]](#)
- Cong, Y.; Kang, H.; Yan, G. Investigation of dynamic behavior of a cable-stayed cantilever beam under two-frequency excitations. *Int. J. Non-Linear Mech.* **2021**, *129*, 103670. [\[CrossRef\]](#)

22. Jalali, M.H.; Rideout, G. Analytical and experimental investigation of cable–beam system dynamics. *J. Vib. Control* **2019**, *25*, 2678–2691. [[CrossRef](#)]
23. Paolo, L.; Arturo, P. A numerical study on the structural integrity of self-anchored cable-stayed suspension bridges. *Frat. Integrità Strutt.* **2016**, *38*, 359–376. [[CrossRef](#)]
24. Zhou, Y.; Chen, S. Investigation of the Live-Load Effects on Long-Span Bridges under Traffic Flows. *J. Bridge Eng.* **2018**, *23*, 101–118. [[CrossRef](#)]
25. Fujino, Y.; Warnitchai, P.; Pacheco, B.M. Experimental and analytical study of autoparametric resonance in a 3DOF model of cable-stayed-beam. *Nonlinear Dyn.* **1993**, *4*, 111–138. [[CrossRef](#)]
26. Ma, C.M.; Duan, Q.S.; Liao, H.L. Experimental Investigation on Aerodynamic Behavior of a Long Span Cable-stayed Bridge Under Construction. *KSCE J. Civ. Eng.* **2018**, *22*, 2492–2501. [[CrossRef](#)]
27. Yang, Y.; Wang, X.; Wu, Z. Experimental Study of Vibration Characteristics of FRP Cables for Long-Span Cable-Stayed Bridges. *J. Bridge Eng.* **2015**, *20*, 04014074. [[CrossRef](#)]

Disclaimer/Publisher’s Note: The statements, opinions and data contained in all publications are solely those of the individual author(s) and contributor(s) and not of MDPI and/or the editor(s). MDPI and/or the editor(s) disclaim responsibility for any injury to people or property resulting from any ideas, methods, instructions or products referred to in the content.